www.nature.com/aps

Acta Pharmacologica Sinica

ARTICLE

Increased intracellular Cl^- concentration mediates neutrophil extracellular traps formation in atherosclerotic cardiovascular diseases

Hui Han[1], Chang Liu[1], Mei Li[2], Jin Wang[3], Yao-sheng Liu[1], Yi Zhou[3], Zi-cheng Li[1], Rui Hu[1], Zhi-hong Li[1], Ruo-mei Wang[4], Yong-yuan Guan[1], Bin Zhang[2] and Guan-lei Wang[1]

Neutrophil extracellular traps (NETs) play crucial roles in atherosclerotic cardiovascular diseases such as acute coronary syndrome (ACS). Our preliminary study shows that oxidized low-density lipoprotein (oxLDL)-induced NET formation is accompanied by an elevated intracellular Cl^- concentration ($[Cl^-]_i$) and reduced cystic fibrosis transmembrane conductance regulator (CFTR) expression in freshly isolated human blood neutrophils. Herein we investigated whether and how $[Cl^-]_i$ regulated NET formation in vitro and in vivo. We showed that neutrophil $[Cl^-]_i$ and NET levels were increased in global *CFTR* null (*Cftr*$^{-/-}$) mice in the resting state, which was mimicked by intravenous injection of the CFTR inhibitor, $CFTR_{inh}$-172, in wild-type mice. OxLDL-induced NET formation was aggravated by defective CFTR function. Clamping $[Cl^-]_i$ at high levels directly triggered NET formation. Furthermore, we demonstrated that increased $[Cl^-]_i$ by $CFTR_{inh}$-172 or *CFTR* knockout increased the phosphorylation of serum- and glucocorticoid-inducible protein kinase 1 (SGK1) and generation of intracellular reactive oxygen species in neutrophils, and promoted oxLDL-induced NET formation and pro-inflammatory cytokine production. Consistently, peripheral blood samples obtained from atherosclerotic *ApoE*$^{-/-}$ mice or stable angina (SA) and ST-elevation ACS (STE-ACS) patients exhibited increased neutrophil $[Cl^-]_i$ and SGK1 activity, decreased *CFTR* expression, and elevated NET levels. VX-661, a CFTR corrector, reduced the NET formation in the peripheral blood sample obtained from oxLDL-injected mice, *ApoE*$^{-/-}$ atherosclerotic mice or patients with STE-ACS by lowering neutrophil $[Cl^-]_i$. These results demonstrate that elevated neutrophil $[Cl^-]_i$ during the development of atherosclerosis and ACS contributes to increased NET formation via Cl^--sensitive SGK1 signaling, suggesting that defective CFTR function might be a novel therapeutic target for atherosclerotic cardiovascular diseases.

Keywords: atherosclerotic cardiovascular diseases; neutrophil extracellular traps; intracellular chloride; CFTR; oxLDL; SGK1

Acta Pharmacologica Sinica (2022) 43:2848–2861; https://doi.org/10.1038/s41401-022-00911-9

INTRODUCTION

The formation of neutrophil extracellular traps (NETs) from activated neutrophils was originally discovered as a part of the first line of host defense against microbial invasion in infectious diseases. In response to a wide variety of stimuli, neutrophils release NETs that contain histones, nuclear proteases, and granular enzymes through which neutrophils can entrap microbial pathogens. Recent accumulating pieces of evidence demonstrate that NETs are emerging as crucial components of the pathological progression of atherosclerotic cardiovascular diseases, including acute coronary syndrome (ACS) [1–4]. ACS is a critical and severe form of cardiovascular diseases with high fatality rate caused by unstable coronary atherosclerotic plaque rupture or invasion and secondary to thrombosis formation, which includes unstable angina, non-ST elevated ACS and ST-elevated ACS, but the precise pathomechanism of ACS is still unclear. An analysis of coronary thrombus and coronary plasma samples obtained from patients with ST-elevation ACS (STE-ACS) revealed that the thrombus NET burden (as detected via biomarkers of NETs, i.e., double-stranded DNA [dsDNA], myeloperoxidase [MPO], neutrophil elastase [NE], or histone levels) in culprit arteries was negatively correlated with ST-segment resolution and positively correlated with infarct size and the occurrence of in-hospital major adverse cardiovascular events, suggesting that NETs have a predictive role in ACS [3]. NETs induce and promote prothrombotic disorder and a proinflammatory milieu among patients with cardiovascular diseases. Therefore, therapeutic compounds targeting NET formation (such as reactive oxygen species [ROS] scavengers, deoxyribonuclease [DNase] therapeutic agents, and peptidylarginine deiminase 4 [PAD4] inhibitors) are in development [4]. Understanding the mechanism underlying NET formation at a molecular level should help identify novel potential targets for the treatment of cardiovascular disease.

Abnormal chloride (Cl^-) transport has been proposed to contribute to the pathogenesis of cardiovascular diseases [5, 6].

[1]Department of Pharmacology, Cardiac and Cerebral Vascular Research Center, Zhongshan School of Medicine, Sun Yat-sen University, Guangzhou 510080, China; [2]VIP Healthcare Center, the Third Affiliated Hospital of Sun Yat-sen University, Guangzhou 510630, China; [3]Guangdong Cardiovascular Institute, Guangdong Provincial People's Hospital, Guangdong Academy of Medical Sciences, Guangzhou 510080, China and [4]School of Data and Computer Science, Sun Yat-sen University, Guangzhou 510006, China
Correspondence: Bin Zhang (drbinzhang@163.com) or Guan-lei Wang (wangglei@mail.sysu.edu.cn)
These authors contributed equally: Hui Han, Chang Liu, Mei Li.

Received: 19 October 2021 Accepted: 7 April 2022
Published online: 5 May 2022

For example, low serum Cl^- level has been implicated as an independent predictor of mortality among patients with heart failure and pulmonary arterial hypertension [7, 8]. Alteration in the intracellular Cl^- concentration ($[Cl^-]_i$) in neutrophil is crucial to neutrophil degranulation and intraphagolysosomal production of hypochlorous acid (HOCl) [9, 10], a potent ROS responsible for the antimicrobial activity of phagosomes. Obvious changes in $[Cl^-]_i$ have also been found in cerebrovascular smooth muscle cell proliferation and airway epithelial inflammation in patients with bronchiectasis [11, 12]. Recent studies of airway epithelial cells demonstrated that increased $[Cl^-]_i$ induces Cl^--sensitive signaling pathways and NF-κB activation and thus promotes airway inflammation, suggesting an emerging role for $[Cl^-]_i$ regulation in pathological processes [12]. However, it is unclear whether the alteration in neutrophil $[Cl^-]_i$ can induce NET formation.

Mutations in the cystic fibrosis transmembrane conductance regulator (*CFTR*) gene, cause cystic fibrosis (CF), a recessively inherited and lethal disease among Caucasians. *CFTR* encodes a cAMP-dependent Cl^- channel. In CF, neutrophils display a delay in apoptosis that is associated with the disrupted CFTR function, and the delayed neutrophil apoptosis in CF causes increased NET production and in turn, promotes inflammation. Treatment with ivacaftor (a CFTR potentiator) could reverse the survival defect, suggesting that the CFTR Cl^- channel plays a role in NET formation by regulating apoptotic pathways [13]. However, whether CFTR-dependent $[Cl^-]_i$ changes during NET formation and how $[Cl^-]_i$ regulates NETs remain unknown. There is no evidence as yet to indicate the pathophysiological significance of the alteration in $[Cl^-]_i$ in relation to NET formation under pathological conditions.

In this study, we initially observed that oxidized low-density lipoprotein (oxLDL)-induced NET formation was accompanied by elevated $[Cl^-]_i$ and decreased CFTR protein expression in freshly isolated human blood neutrophils. We, therefore, hypothesized that the alteration in $[Cl^-]_i$ resulting from *CFTR* deficiency may play an important role in NET formation associated with atherosclerotic cardiovascular diseases. Our results demonstrated that CFTR is a Cl^- channel responsible for the elevated neutrophil $[Cl^-]_i$ during the increased formation of NETs associated with atherosclerotic cardiovascular diseases by using global *CFTR* knockout mice intravenously injected with oxLDL. Moreover, our mechanistic analysis revealed that serum- and glucocorticoid-regulated kinase (SGK1) is activated by elevated neutrophil $[Cl^-]_i$ and *CFTR* deficiency and thereby potentiates NET formation via intracellular ROS production. We also examined whether CFTR dysfunction, neutrophil $[Cl^-]_i$, and Cl^--sensitive SGK1 signaling are associated with increased peripheral blood NET burden in atherosclerotic $ApoE^{-/-}$ mice or stable angina (SA) and STE-ACS patients.

MATERIALS AND METHODS

Animals

The protocols of all experimental procedures were approved by the Sun Yat-sen University Animal Care and Use Committee (approval No. SYSU-IACUC-2020-000446). All procedures were performed following the "Guide for the Care and Use of Laboratory Animals" issued by the Ministry of Science and Technology of China.

$CFTR^{tm1Unc\text{-}Tg\ (FABPCFTR)\ 1Jaw/J}$ knockout ($Cftr^{-/-}$) mice were purchased from the Jackson Laboratory (Bar Harbor, ME, USA) [14]. The wild-type (*Wt*) C57BL/6J mice and $Cftr^{-/-}$ mice used in the present study were 8–16 weeks old and weight-matched. C57BL/6J mice were obtained from the Laboratory Animal Center of Sun Yat-sen University (Guangzhou, China) and intravenously injected with the selective CFTR inhibitor, $CFTR_{inh}$-172 (2 mg/kg; Sigma–Aldrich Co. LLC., MO, USA) 24 h before the experiments. Mice injected with the same volume of saline containing dimethylsulfoxide (final concentration <0.1%; Sigma-Aldrich) served as controls. The doses of $CFTR_{inh}$-172 and oxLDL were selected based on previous reports [15] and the exacerbating effects of both reagents on NET formation were confirmed in our preliminary experiments.

Atherosclerotic $ApoE^{-/-}$ mice were prepared as we previously described [16]. Male $ApoE^{-/-}$ mice were purchased from the GemPharmatech Co., Ltd. (Guangzhou, China). All the mice were housed in microisolator cages under conditions of controlled temperature (23–26 °C) and humidity (60%) with a 12-h light/dark cycle with free access to standard chow and sterile water. After 1 week of acclimatization to the environment, $ApoE^{-/-}$ mice were switched to a high-fat diet (HFD, formulation: 45% of total calories from fat [D12079B]) for 16 weeks, while healthy male C57BL/6J mice received a HFD and served as controls. After 16 weeks, all the mice were sacrificed. Peripheral blood samples were collected for biochemical analysis.

Patient characterization

The study was conducted following the Declaration of Helsinki. The study protocol was approved by the Ethics Committee of the Sun Yat-sen University (approval No. 2020-024) and the Ethics Committee of Guangdong Provincial People's Hospital (approval No. KY-2020-062-01-02). All individuals were enrolled from Guangdong Provincial People's Hospital and divided into the STE-ACS, stable angina (SA), and normal coronary artery (NCA) groups according to the diagnostic criteria applied after coronary angiography. All patients provided written informed consent before enrollment. All participant details are indicated in Supplementary Table S1. A total of 90 patients were enrolled, including 36 patients with STE-ACS, 23 with SA, and 31 with NCA.

STE-ACS is acute coronary syndrome (ACS) with ST elevation. For patients with STE-ACS, the following inclusion criteria had to be met: (i) characteristic clinical symptoms; (ii) chest pain at the time of coronary angiography; (iii) electrocardiographic ST-elevation; and (iv) coronary anatomy suitable for thrombectomy.

SA is defined as symptoms that may be ascribed to myocardial ischemia, for example, paroxysmal and episodic chest discomfort induced by myocardial ischemia, which lasts from a few minutes to 10 more minutes, but no more than half-hour. For patients with SA, the following inclusion criteria had to be met: (i) characteristic chest pain; (ii) caused by physical or psychological stress; and (iii) relieved after rest or nitroglycerine, with typical angina requiring all three criteria fulfilled, atypical angina two criteria and the presence of coronary angiograph was defined as site interpretation of >70% area stenosis in any major epicardial vessel or >50% stenosis in the left main stem.

The exclusion criteria for patients with STE-ACS or SA included the following: (i) need for chronic oral anticoagulant therapy, chronic low-molecular-weight heparin, or long-term treatment with fondaparinux; (ii) age <18 years; (iii) renal disease; (iv) hepatic disease; (v) pregnancy or lactation; (vi) advanced cancer or hemodialysis; (vii) severe inflammatory disease or immune disorder; (viii) history of thrombocytopenia or neutropenia; and (ix) patients considered to be at risk of bradycardic events.

Isolation and purification of neutrophils

Human peripheral blood samples were obtained via venipuncture at Guangdong Provincial People's Hospital and neutrophils were isolated as described previously [17]. Briefly, freshly obtained peripheral blood samples from healthy adult donors and patients were collected in heparinized tubes and layered onto separating solution (Beijing Solarbio Science and Technology Co., Ltd., Beijing, China), and then centrifuged at $1000 \times g$ for 30 min. The neutrophil layer was retrieved and washed with phosphate-buffered saline (PBS). Red blood cells were removed using red blood cell lysis buffer. Neutrophils were washed twice with PBS, resuspended in Roswell Park Memorial Institute Medium 1640 (2.0×10^6 cells/mL), and incubated at 37 °C and in 5% carbon

dioxide (CO_2) for at least 30 min before use. At least 95% of cell populations were obtained in this way and were subjected to immunofluorescence staining analysis with anti-Ly6G antibody (Abcam PLC., Cambridge, UK).

Intracellular Cl^- level measurement

$[Cl^-]_i$ was assessed using *N*- (ethoxycarbonylmethyl)-6-methoxyquinolinium bromide (MQAE) according to a previously reported procedure with slight modifications [12]. Briefly, neutrophils were incubated with 5 mM of MQAE (Invitrogen, MA, USA) for 30 min at 37 °C in the dark, then washed with Krebs HEPES (128 mM NaCl, 5 mM KCl, 1 mM $MgSO_4{\cdot}7H_2O$, 15 mM glucose, 20 mM HEPES, 2 mM $CaCl_2$, 296–298 mM mOsm, pH 7.4) before measurement. Fluorometric data were obtained at 37 °C using a spectrofluorometer (SpectraMax M5; Molecular Devices Corporation, CA, USA) at excitation and emission wavelengths of 355 and 460 nm, respectively. The cells were permeabilized using tributyltin (10 μM) and nigericin (7 μM) in a high-K^+ solution. The calibration curve was obtained by fitting fluorescence intensity corresponding to known Cl^- concentrations, and the neutrophil $[Cl^-]_i$ was calculated accordingly.

Isolation and culture of human umbilical vein endothelial cells

Human umbilical vein endothelial cells (HUVECs) were isolated and cultured as we described previously [18]. Briefly, HUVECs were removed from human umbilical veins after collagenase type I digestion, and maintained at 37 °C in a 5% CO_2 humidified atmosphere in medium 199 containing 20% fetal calf serum, penicillin (100 U/mL), streptomycin (100 U/mL), and heparin (50 U/mL), supplemented with *L*-glutamine (2 mM), sodium pyruvate (1 mM), and beta-endothelial cell growth factor (5 ng/mL), on 0.1% gelatin-coated culture flasks. Endothelial cells were identified by their "cobblestone" mosaic appearance when reaching confluence and the presence of the von Willebrand factor. Endothelial cell passages between three and six were used in the present study.

Measurement of the plasma dsDNA level

The plasma dsDNA level was quantified using the Quant-iT™ PicoGreen® dsDNA Assay Kit (Invitrogen) according to the manufacturer's protocol. Briefly, the diluted plasma was mixed with PicoGreen Reagent in a 96-well plate, and the dsDNA level was measured using a SpectraMax M5 microplate reader (Molecular Devices Corporation) at excitation and emission wavelengths of 485 and 525 nm, respectively [19–22].

Enzyme-linked immunosorbent assay

Highly sensitive C-reactive protein (hs-CRP) and proinflammatory cytokines (TNF-α, IL-1β, and IL-6) and NET-associated proteins such as MPO and NE in human or mouse plasma were quantified using an enzyme-linked immunosorbent assay (ELISA) kit (MLBio; Shanghai Enzyme-Linked Biotechnology Co., Ltd., Shanghai, China) according to the manufacturer's instructions. For instance, plasma samples were placed into 96-well plates coated with mouse anti-human MPO antibody after blocking with 1% casein, followed by incubation with horseradish peroxide-labeled anti-MPO monoclonal antibody and color development using 3,3′,5,5′-tetramethylbenzidine substrate. The optical absorbance was measured using a Sunrise™ ELISA plate reader (Tecan, Austria) at 450 nm. The standard curve was obtained by plotting the average optical density of the standard samples along the *Y*-axis versus the corresponding concentration on the *X*-axis. Plasma MPO levels were then determined by comparing the optical density of the samples to the standard curve [23].

Fluorescent image analysis of NETs

After the neutrophils were stimulated with oxLDL for 4 h at 37 °C in 5% CO_2, the oxLDL-treated neutrophils were washed with PBS and fixed with 4% paraformaldehyde for 15 min at room temperature. After blocking with an Immunol Staining Blocking Buffer (Beyotime Biotechnology, Shanghai, China) for 1 h at room temperature, the cells were incubated with anti-human MPO antibody (Abcam PLC) at room temperature for 1 h (or at 4 °C overnight), followed by a fluorescein isothiocyanate-labeled secondary antibody (Life Technologies Corporation, CA, USA) for 1 h and then 4′,6-diamidino-2-phenylindole (Sigma-Aldrich) for another 5 min at room temperature. The cells were washed thrice in PBS prior to microscopy. NET formation was then observed under a fluorescent microscope (Carl Zeiss Meditec AG, Oberkochen, Germany) [24].

Flow cytometric analysis

To detect the expression of CFTR protein on neutrophils, neutrophils were resuspended with 100 μL of 1% bovine serum albumin (BSA)-PBS (containing 0.09% sodium azide as a metabolic inhibitor). To block Fc receptors, the cell suspension was incubated with FcBlock in Staining Buffer (BD Biosciences, NJ, USA) for 15 min on ice and then incubated with anti-CFTR antibody (Novus Biologicals, CO, USA) for another 20 min in the dark at room temperature. After incubation with primary antibody, the cell pellets were resuspended in 1% BSA-PBS and incubated with Alexa Fluor 647 labeled-Donkey anti-Rabbit IgG (H + L) Highly Cross-Adsorbed Secondary Antibody (Thermo Fisher Scientific, MA, USA) for 20 min in the dark at 4 °C. The background fluorescence was quantified using an Alexa Fluor® 647 IgG κ isotype control (BioLegend, CA, USA). Cells were then assessed using a Beckman Coulter Gallios Flow Cytometer and analyzed using the Kaluza software (Beckman Coulter, Inc., CA, USA) [25].

Western blotting assay

Neutrophils were harvested using radioimmunoprecipitation assay buffer (Beyotime Biotechnology) and immunoblots were performed as previously described [26]. Briefly, the samples were separated by 8% sodium dodecyl sulfate-polyacrylamide gel electrophoresis and then transferred to a nitrocellulose membrane. The membrane was incubated with the corresponding primary antibodies overnight, followed by the appropriate horseradish peroxidase-conjugated secondary antibodies for 1.5 h. The bands were detected using an enhanced chemiluminescence detection system (Beyotime Biotechnology). Chemiluminescence images were captured using an imaging system (Bio-Rad Laboratories, Inc., CA, USA). The optical densities were normalized to those of glyceraldehyde 3-phosphate dehydrogenase (GAPDH), and the fold difference for each target protein was calculated as the ratio of the target protein expression/GAPDH expression (using ImageJ version 1.42q; National Institutes of Health, MD, USA). The following primary antibodies were used: anti-CFTR (1:200; Novus Biologicals), anti-histone H3 (citrulline R17) (1:1000; Abcam PLC), anti-NF-κB (1:1000; Cell Signaling Technology, MA, USA), anti-p-NF-κB (1:1000; Cell Signaling Technology), anti-SGK1 (1:500; Santa Cruz Biotechnology Inc., CA, USA), anti-p-SGK1 (1:500; Santa Cruz Biotechnology), and anti-GAPDH (1:2000; Cell Signaling Technology).

Detection of intracellular ROS

Intracellular ROS was detected as we described previously [18]. Briefly, intracellular ROS levels were measured via flow cytometry using 2′,7′-dichlorodihydrofluorescein diacetate (DCFH-DA; Dalian Meilun Biotechnology Co., Ltd., Dalian, China) as a ROS-sensitive fluorescence probe. DCFH formed within cells would be oxidized by intracellular ROS and converted to DCF; thus, the detected fluorescent signal would be proportional to ROS production. In the present study, neutrophils (2×10^6/mL) were loaded with DCFH-DA. Following 30 min of incubation, the reaction was terminated by chilling samples on ice and the fluorescence intensity was immediately measured via flow cytometry (Beckman Coulter, Inc.).

Statistical analysis

All data are expressed as means ± SEM (Standard Error of Mean). The statistical analyses were performed using SPSS Statistics version 25.0 (IBM Corporation, NY, USA). The unpaired Student *t* test was used to compare two groups. Three or more groups were compared via one-way analysis of variance, followed by Bonferroni's multiple comparison post hoc test and the results expressed in terms of 95% confidence intervals. Analysis items with $P < 0.05$ were considered statistically significant.

RESULTS

OxLDL increased $[Cl^-]_i$ in neutrophils during NET formation

NET formation was induced among human peripheral blood neutrophils isolated from healthy donors and incubated with 100 μg/mL of oxLDL for 4 h, as described previously (Fig. 1a, b) [27]. OxLDL induces the loss of the typical segmented nuclear morphology, formation of the DNA fiber network structure, and increased citrullinated histone H3 (CitH3) protein expression in neutrophils, as detected via confocal microscopy and Western blot analysis. CFTR protein expression was significantly decreased in neutrophils from the oxLDL-treated group compared with those from the control group, as detected via immunofluorescence staining (Fig. 1c). We next measured whether the $[Cl^-]_i$ in neutrophils changed during oxLDL-induced NET formation. The analysis with MQAE demonstrated that treatment with 100 μg/mL oxLDL for 30 min significantly increased the $[Cl^-]_i$ in human neutrophils from 63.1 ± 0.6 to 72.9 ± 0.5 mM (Fig. 1d).

Higher neutrophil $[Cl^-]_i$ induces NET formation

The observation of elevated $[Cl^-]_i$ in neutrophils with oxLDL-induced NET formation led us to investigate whether alteration of $[Cl^-]_i$ could modulate NET formation. We established an in vitro model with gradients of $[Cl^-]_i$ in neutrophils by changing extracellular Cl^- concentrations as previously described (Fig. 1e) [12]. The $[Cl^-]_i$ could instantaneously reach the same level as the extracellular Cl^- concentration upon perfusion with 0, 30, 70, and 100 mM of Cl^-. Neutrophil MPO and NE levels were upregulated by increasing $[Cl^-]_i$ in neutrophils in a concentration-dependent manner (Fig. 1f). There were no significant differences in MPO and NE levels among neutrophils between the groups with $[Cl^-]_i$ of 0 and 30 mM. When the $[Cl^-]_i$ was elevated to 70 and 100 mM, MPO and NE levels increased significantly compared with that of the group with an $[Cl^-]_i$ of 0 mM. CitH3 protein expression (Fig. 1g) and the release of dsDNA from the supernatant (Fig. 1h) increased in the group with an $[Cl^-]_i$ of 100 mM in a time-dependent manner. These data indicated that increasing the $[Cl^-]_i$ in neutrophils could directly induce NET formation.

Increased neutrophil $[Cl^-]_i$ secondary to *CFTR* deficiency promotes oxLDL-induced NET formation

CFTR mediates transmembrane Cl^- outflow and regulates the $[Cl^-]_i$ in cells. We, therefore, hypothesized that *CFTR* deficiency may cause Cl^- outflow obstruction, which would in turn increase $[Cl^-]_i$ and NET formation. We next examined the effects of *CFTR* deficiency on neutrophil $[Cl^-]_i$ during NET formation in mice with global *CFTR* knockout ($Cftr^{-/-}$). The $[Cl^-]_i$ of $Cftr^{-/-}$ neutrophils was significantly higher than that of wild-type (C57BL/6J) neutrophils in the resting state (71.7 ± 0.5 *vs* 66.1 ± 0.4 mM) (Fig. 2a). Consistent with a previous report [13], $Cftr^{-/-}$ neutrophils formed more NETs than corresponding C57BL/6J controls. ELISA showed that neutrophils isolated from $Cftr^{-/-}$ mice released higher MPO and NE levels than those isolated from the C57BL/6J mice (Fig. 2b). Immunofluorescence images of MPO showed similar results (Fig. 2c). These results suggested that abnormal heightened neutrophil $[Cl^-]_i$ secondary to *CFTR* deficiency may play a role in NET formation.

As a CFTR Cl^- channel blocker, $CFTR_{inh}$-172 inhibits CFTR Cl^- channel-mediated Cl^- transport by binding to the nucleotide-binding domains of CFTR protein rather than affecting CFTR protein expression. Consistent with the results obtained from $Cftr^{-/-}$ mice, pharmacological inhibition of the CFTR Cl^- channel with 2 mg/kg $CFTR_{inh}$-172 in C57BL/6 J mice also increased neutrophil $[Cl^-]_i$ and dsDNA release (Fig. 2d, e). Incubating healthy human circulating neutrophils with $CFTR_{inh}$-172 (0.5, 1, 2.5, and 5 μM) increased CitH3 protein expression and dual acridine orange/ethidium bromide fluorescent staining of dsDNA in a concentration-dependent manner (Fig. 2f, g). These results indicate cell type-specific regulation of CFTR-dependent $[Cl^-]_i$ in neutrophils and NET formation. Taken together, these data indicate that genetic interventions involving *CFTR* or pharmacological inhibition of CFTR Cl^- channels increase neutrophil $[Cl^-]_i$ and promote NET formation in vivo and in vitro.

We further investigated the effects of *CFTR* deficiency on oxLDL-induced blood NET formation in $Cftr^{-/-}$ mice intravenously injected with oxLDL. We demonstrated that in vivo administration of oxLDL induced increases in plasma MPO, NE, dsDNA, and proinflammatory cytokine (IL-1β, IL-6, and hs-CRP) levels (Supplementary Fig. S2a–c). Compared to the control mice, $Cftr^{-/-}$ mice injected with oxLDL exhibited a further increase in peripheral blood NET formation as evidenced by significantly higher levels of plasma MPO, NE, and dsDNA (Fig. 3a, b). Plasma levels of proinflammatory biomarkers or cytokines (hs-CRP and IL-1β) were further increased in oxLDL-injected $Cftr^{-/-}$ mice compared to corresponding saline-injected $Cftr^{-/-}$ mice (Fig. 3c), while there was no significant difference in IL-6 level between oxLDL-injected $Cftr^{-/-}$ mice and corresponding control mice (Fig. 3c). The above results indicated that the loss of *CFTR* further enhanced NET formation and promoted oxLDL-induced inflammation. Of note, $Cftr^{-/-}$ neutrophils showed increased basal $[Cl^-]_i$, which was further augmented by oxLDL (72.1 ± 0.6 vs 75.9 ± 0.4 mM) (Fig. 3d).

Given that loss of *CFTR* increases neutrophil $[Cl^-]_i$ and promotes oxLDL-induced NET formation and production of inflammatory cytokines, we hypothesized that clinical use of the CFTR corrector, VX-661 [9], may reduce the oxLDL-induced increase in neutrophil $[Cl^-]_i$ and NET formation and inflammation by improving processing and trafficking of CFTR Cl^- channels to the cell membrane. The oxLDL-induced increases in neutrophil $[Cl^-]_i$ and plasma MPO and NE levels were significantly reduced via intravenous injection of 2 mg/kg VX-661 before stimulation with oxLDL (Fig. 3e, f). VX-661 administration also significantly reduced oxLDL-induced production of inflammatory mediators, including hs-CRP and IL-1β (Fig. 3g). Furthermore, preincubation of freshly isolated wild-type (*Wt*) mouse neutrophils with 5 μM VX-661 for 30 min significantly abrogated the increased $[Cl^-]_i$ in neutrophil and NET formation induced by oxLDL in vitro (Fig. 3h, i). Collectively, these findings indicated that oxLDL potently increased neutrophil $[Cl^-]_i$, NET formation, and production of proinflammatory mediators, which were attenuated by a CFTR corrector, but were further potentiated by genetic ablation of *CFTR* or pharmacological inhibition of CFTR Cl^- channels, suggesting that CFTR-mediated neutrophil $[Cl^-]_i$ dynamics play an important role in regulating oxLDL-induced NET formation; while controlling neutrophil $[Cl^-]_i$ would retard oxLDL-induced NET formation.

Higher neutrophil $[Cl^-]_i$ activates SGK1 and ROS production during NET formation

SGK1 has been identified as a Cl^--sensitive kinase in a variety of cell types including vascular smooth muscle cells and airway epithelial cells. We thus assessed whether SGK1 could be activated by elevated $[Cl^-]_i$ during NET formation. Neutrophil SGK1 was activated instantly (as shown by phosphorylation at Ser422) when $[Cl^-]_i$ was clamped at a higher level of 100 mM (Fig. 4a). There was no significant difference in total SGK1 protein expression among all groups. Because the loss of *CFTR* increases neutrophil $[Cl^-]_i$, we next confirmed that SGK1 activity is

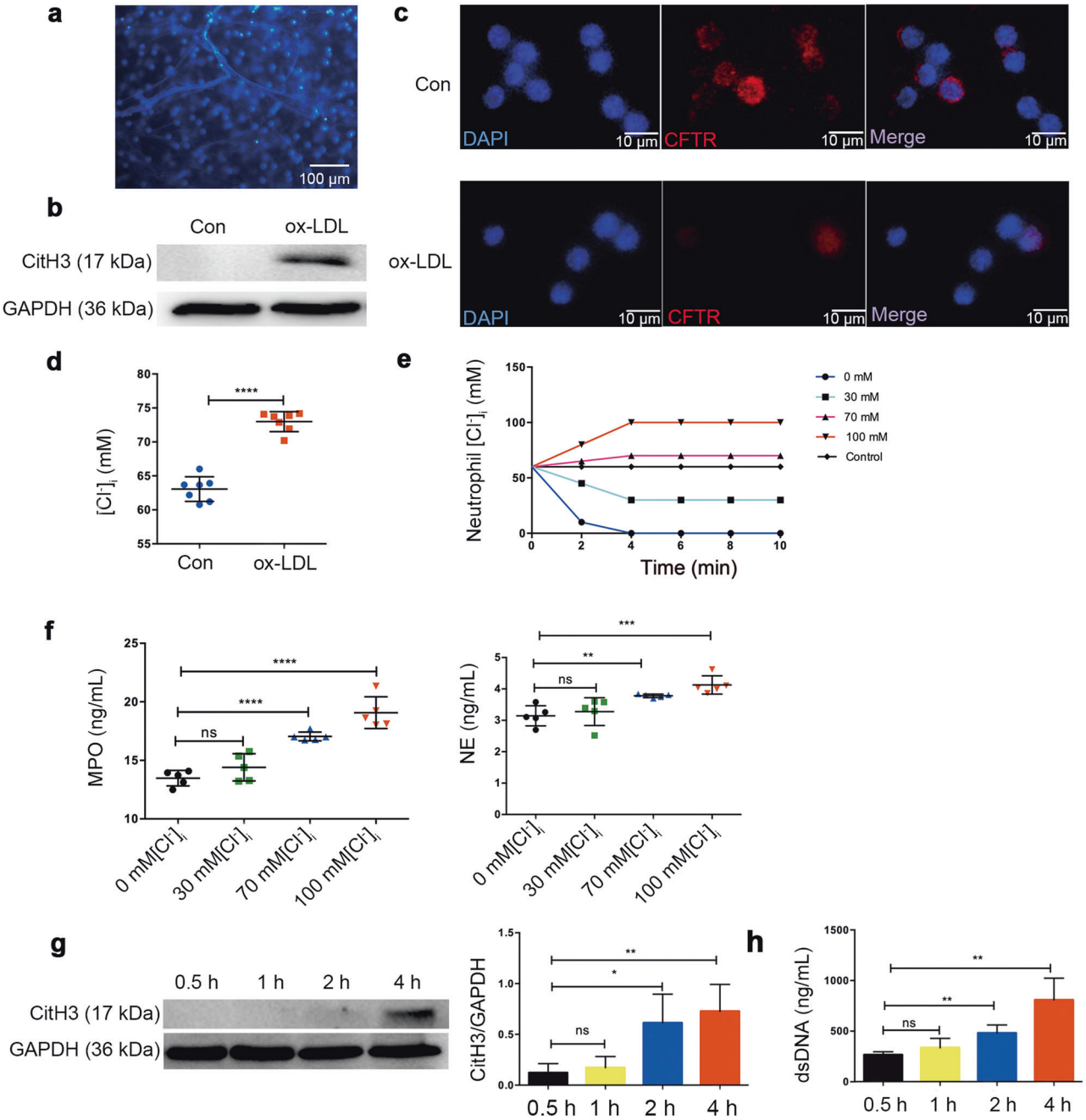

Fig. 1 OxLDL increased $[Cl^-]_i$ and decreased CFTR expression in neutrophils during NET formation, and 100 mM $[Cl^-]_i$ induces NET formation. Neutrophils isolated from the peripheral blood of healthy donors were treated with oxLDL (100 μg/mL) for 4 h to form NETs. **a** Fluorescence staining of DAPI (blue) showing NET structures. Scale bar = 100 μm. **b** Western blotting showing CitH3 protein expression. **c** CFTR expression was analyzed via immunofluorescence staining with Cy3-labeled secondary antibody (red). Scale bar = 10 μm. **d** The $[Cl^-]_i$ was measured using the chloride indicator MQAE probe. **e** In vitro model with gradients of $[Cl^-]_i$ in neutrophils by changing extracellular Cl^- concentrations (0, 30, 70, and 100 mM). **f** ELISA of MPO and NE released from neutrophils in the presence of different $[Cl^-]_i$ (0, 30, 70, and 100 mM). $n = 5$. Isolated neutrophils were stimulated with an $[Cl^-]_i$ of 100 mM to form NETs in a time-dependent manner. CitH3 protein expression was analyzed via Western blotting (**g**) and the release of dsDNA from neutrophils was analyzed using a Pico-Green dsDNA fluorescence probe (**h**). $n = 5$. *ns*, $P > 0.05$; *$P < 0.05$; **$P < 0.01$; ***$P < 0.001$; ****$P < 0.0001$.

upregulated upon exposure to higher $[Cl^-]_i$ in *Cftr*$^{-/-}$ neutrophils compared with corresponding C57BL/6J controls (Fig. 4b). We also confirmed upregulation of SGK1 activity in in vivo and in vitro oxLDL-induced NET formation models (Fig. 4c, d). Since SGK1 has been shown to regulate CFTR-mediated Cl^- transport in nasal mucosal epithelial cells [28], we explored whether SGK1 regulates oxLDL-induced neutrophil CFTR expression and $[Cl^-]_i$ via feedback. Preincubation with GSK650394 (a specific SGK1 inhibitor) abolished in vitro oxLDL-induced NET formation, but did not affect the elevated $[Cl^-]_i$ (Fig. 4e–g). Addition of GSK650394 did not affect elevations in $[Cl^-]_i$ among *Cftr*$^{-/-}$ neutrophils (Fig. 4h).

NET formation is elicited via signaling pathways involving ROS production; we, therefore, examined whether ROS production

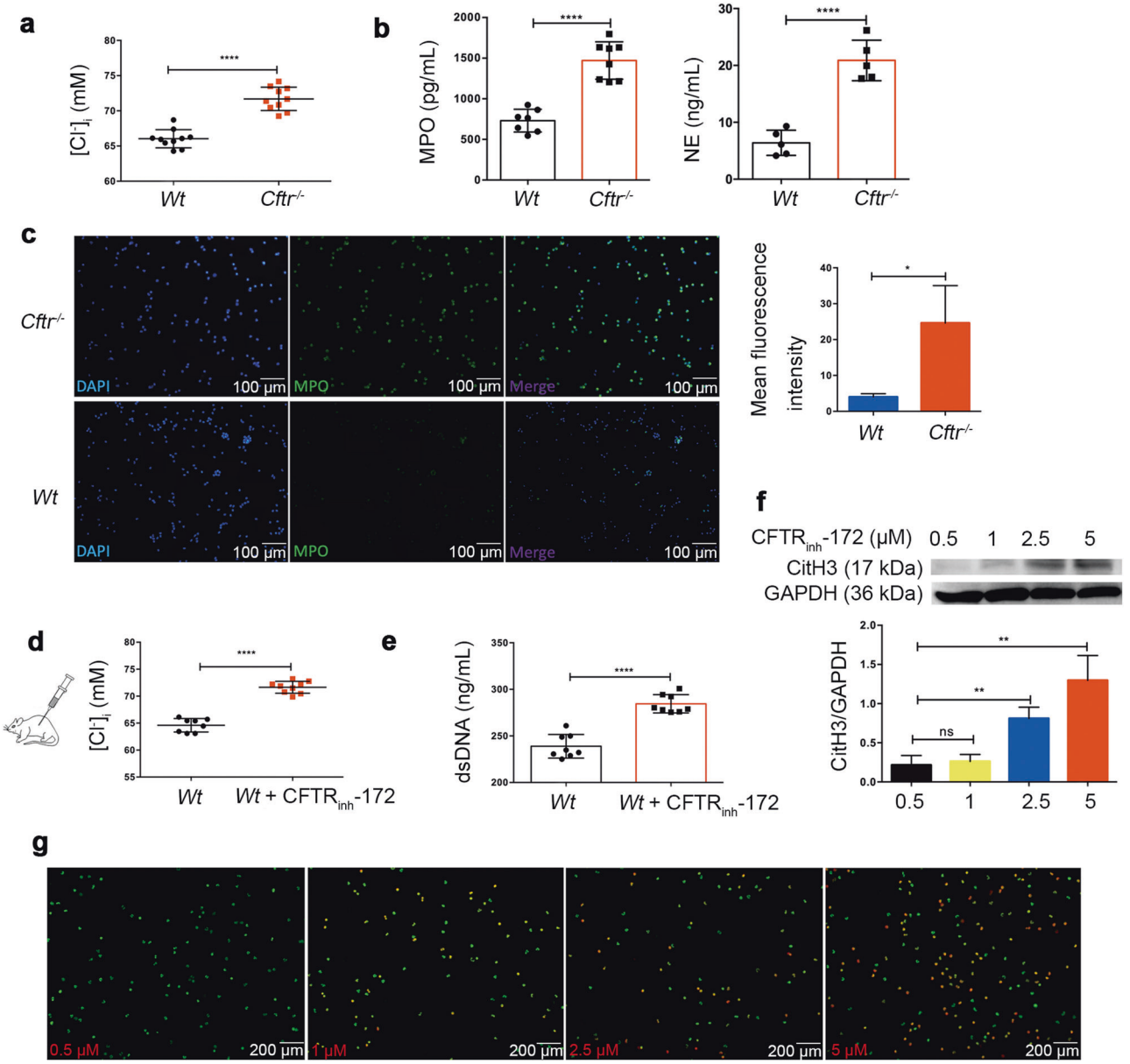

Fig. 2 CFTR dysfunction induces NET formation by regulating neutrophil $[Cl^-]_i$. Neutrophils were isolated from wild-type (*Wt*) mice and *Cftr*$^{-/-}$ mice. **a** Measurement of $[Cl^-]_i$ with an MQAE probe. **b** ELISA of plasma MPO and NE levels in peripheral blood. **c** MPO expression on neutrophils was analyzed by immunofluorescence staining with FITC-labeled secondary antibody (green). Scale bar = 100 μm. **d** Neutrophils in peripheral blood were isolated from *Wt* mice following injection with $CFTR_{inh}$-172 (2 mg/kg) for 24 h. Measurement of $[Cl^-]_i$ with an MQAE probe. **e** Fluorescence probe analysis of plasma dsDNA levels. $n = 8$. **f** Neutrophils isolated from *Wt* mice were treated with different concentrations of $CFTR_{inh}$-172 (0.5, 1, 2.5, and 5 μM) for 4 h to form NETs. Western blotting assay of CitH3 protein. $n = 5$. **g** Neutrophil formation stimulated by $CFTR_{inh}$-172 was analyzed via fluorescence staining with AO/EB (dual acridine orange/ethidium bromide), DNA in neutrophils with complete membrane was stained by AO (green), dsDNA in neutrophil with uncomplete membrane was stained by EB (orange). Scale bar = 200 μm. *ns*, $P > 0.05$; *$P < 0.05$; **$P < 0.01$; ****$P < 0.0001$.

plays a role in NET formation induced by higher $[Cl^-]_i$. Higher $[Cl^-]_i$ (100 mM) significantly enhanced intracellular ROS production in freshly isolated human peripheral blood neutrophils (Fig. 5a). Preincubation with 15 mM N-acetyl cysteine (NAC; an inhibitor of ROS production) for 30 min significantly decreased the increased CitH3 protein expression and dsDNA release induced by higher $[Cl^-]_i$ (Fig. 5b, c). In addition, preincubation with the SGK1 inhibitor, GSK650394, significantly attenuated the increased intracellular ROS production induced by higher $[Cl^-]_i$ (Fig. 5d). Collectively, these results suggested that SGK1 activity regulates NET formation induced by higher $[Cl^-]_i$ by enhancing intracellular ROS production.

Elevated NET formation in peripheral blood of atherosclerotic *ApoE*$^{-/-}$ mice and SA and STE-ACS patients via alteration of neutrophil CFTR, $[Cl^-]_i$, and SGK1 activity

Given that oxLDL-induced increase in neutrophil $[Cl^-]_i$ led to NET formation by regulating the activation of SGK1 and ROS production, we hypothesized that this $[Cl^-]_i$-dependent SGK1 signaling pathway is required for increased NET levels in atherosclerotic disease models with elevated plasma oxLDL levels. We fed C57BL/6J mice and *ApoE*$^{-/-}$ mice with HFD for 16 weeks as we previously described (Supplementary Table S2) [16]. After 16 weeks of HFD, atherosclerotic plaques in the aortic sinus were obvious in *ApoE*$^{-/-}$ mice (Supplementary Fig. S4a, b). The *ApoE*$^{-/-}$

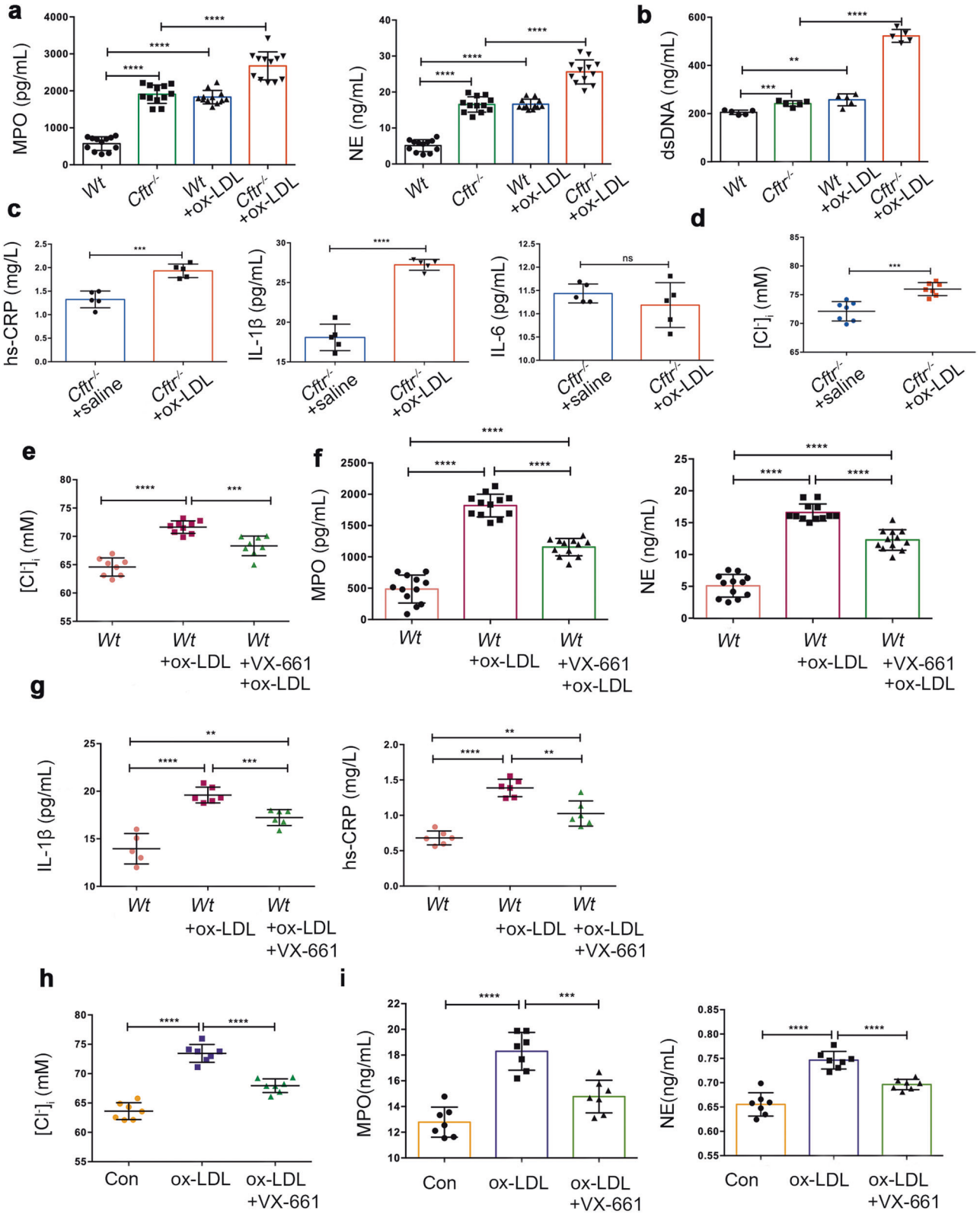

Fig. 3 Increased neutrophil $[Cl^-]_i$ resulting from *CFTR* deficiency aggravates oxLDL-induced NET formation, whereas VX-661 reverses it. *Wt* mice and *Cftr*$^{-/-}$ mice were intravenously injected with 3 mg/kg oxLDL for 24 h. **a** ELISA of plasma MPO and NE levels in peripheral blood. **b** Analysis of plasma dsDNA level using a fluorescence probe. **c** ELISA of plasma levels of hs-CRP, IL-1β, and IL-6. **d** Measurement of $[Cl^-]_i$ with an MQAE probe. $n = 5–12$ mice per group. **e** *Wt* mice were injected with 2 mg/kg VX-661 before the addition of oxLDL for another 24 h. Measurement of $[Cl^-]_i$ with MQAE. ELISA of MPO and NE levels (**f**) or IL-1β and hs-CRP (**g**) levels in plasma. **h** Isolated *Wt* mouse neutrophils were preincubated with VX-661 before stimulation with oxLDL. Measurement of $[Cl^-]_i$ with MQAE. **i** ELISA of MPO and NE levels. $n = 5–12$ mice per group. *ns*, $P > 0.05$; *$P < 0.05$; **$P < 0.01$; ***$P < 0.001$; ****$P < 0.0001$.

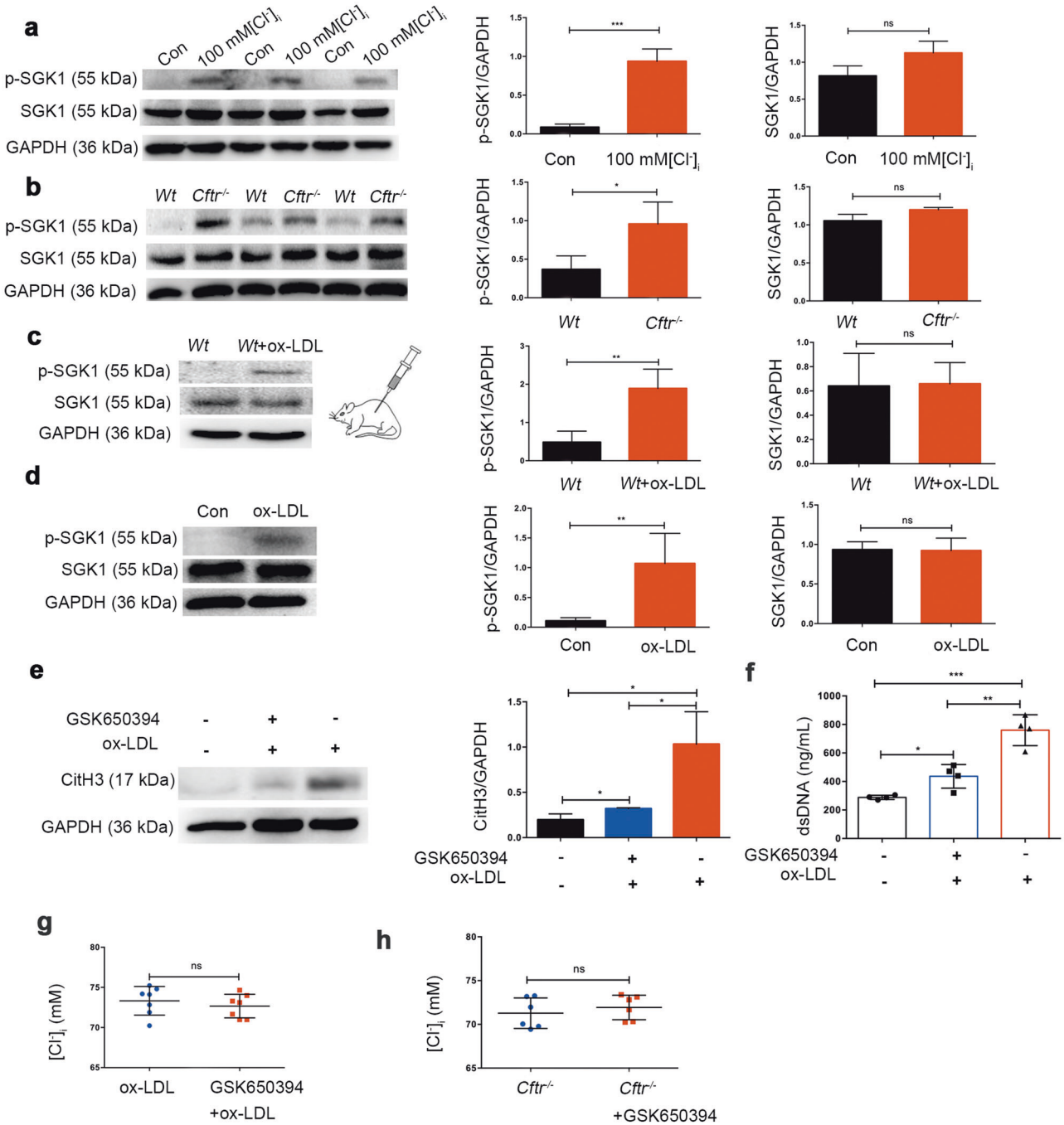

Fig. 4 Phosphorylated SGK1 levels are augmented in neutrophils upon stimulation with high $[Cl^-]_i$ or oxLDL. Western blotting assay of total and phosphorylated SGK1 (S422) in isolated human peripheral blood neutrophils stimulated with an $[Cl^-]_i$ of 100 mM (**a**), or *Cftr*$^{-/-}$neutrophils (**b**), or neutrophils isolated from *Wt* mice injected with oxLDL (**c**), or isolated human peripheral blood neutrophils stimulated with oxLDL (**d**). $n = 5$ independent experiments. (**e**) Neutrophils isolated from *Wt* mice were pre-treated with 1 μM GSK650394 for 30 min before the addition of 100 μg/mL oxLDL for another 4 h. Western blotting assay of CitH3 protein levels. (**f**) Fluorescence probe analysis of dsDNA released from neutrophils. The effect of GSK650394 on $[Cl^-]_i$ of isolated *Wt* mouse neutrophils stimulated with oxLDL (**g**) or $[Cl^-]_i$ of *Cftr*$^{-/-}$neutrophils (**h**). *ns*, $P > 0.05$; *$P < 0.05$; **$P < 0.01$; ***$P < 0.001$, $n = 5$–7 per group.

atherosclerotic mice have higher plasma level of oxLDL compared to that of age-matched HFD C57BL/6J mice (Supplementary Fig. S4c), indicating that we successfully established the *ApoE*$^{-/-}$ atherosclerotic mouse model. $[Cl^-]_i$ and phosphorylated SGK1 protein expression were significantly increased and CFTR protein expression was decreased in circulating neutrophils obtained from *ApoE*$^{-/-}$ mice after a 16-week HFD compared with age-matched HFD C57BL/6J mice (Fig. 6a–c). In line with a previous report [29], the peripheral blood of *ApoE*$^{-/-}$ atherosclerotic mice exhibited a significant increase in plasma NET marker (MPO and NE) and inflammatory marker (IL-1β and hs-CRP) levels (Fig. 6d, e). Moreover, $[Cl^-]_i$ elevation in neutrophils of *ApoE*$^{-/-}$ atherosclerotic mice could be significantly reduced by in vitro VX-661 treatment (Fig. 6f). VX-661 significantly reduced NET formation in peripheral blood samples obtained from *ApoE*$^{-/-}$ atherosclerotic mice (Fig. 6g).

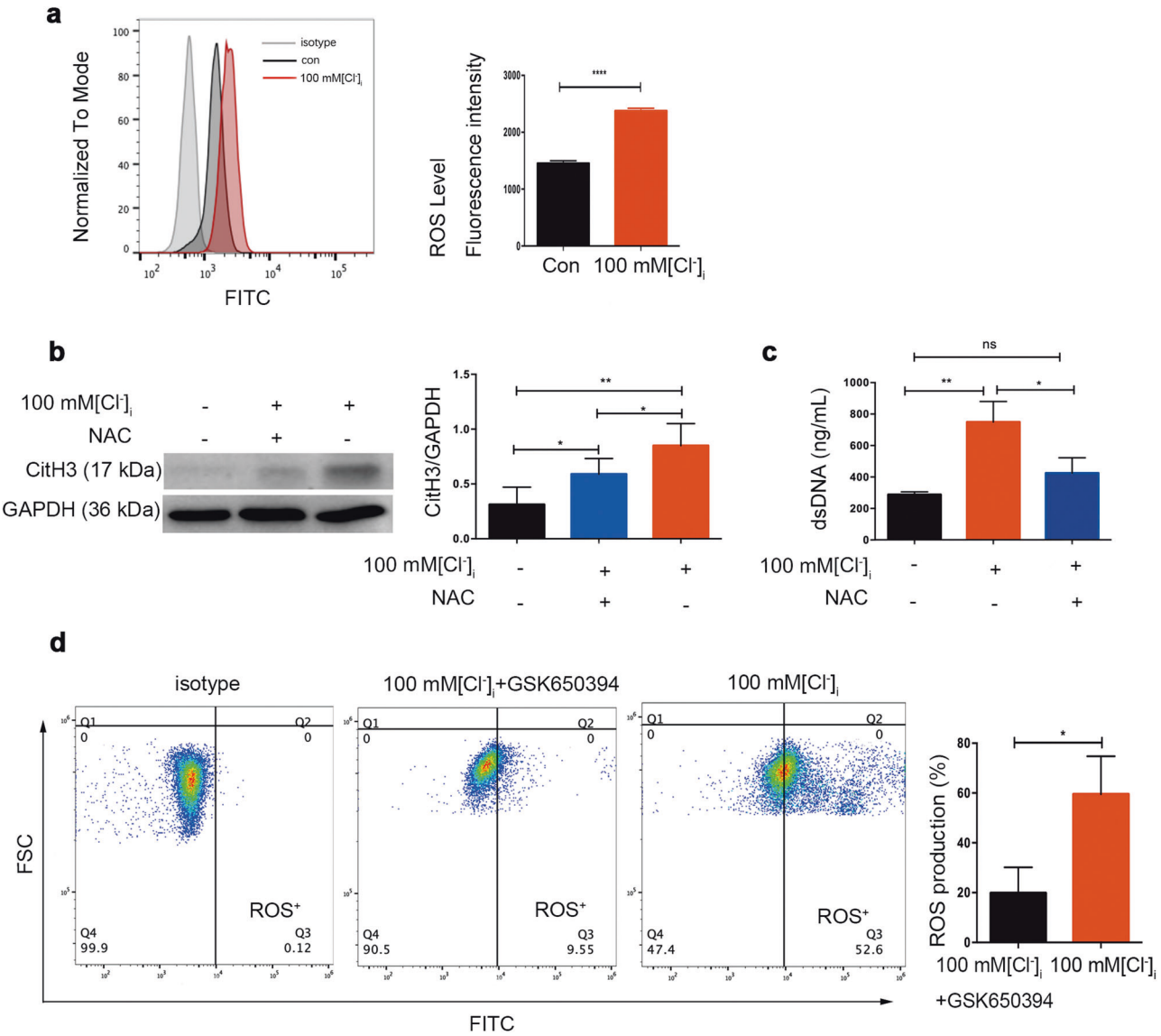

Fig. 5 Higher neutrophil $[Cl^-]_i$ promotes ROS production during NET formation. a The effects of an $[Cl^-]_i$ of 100 mM on intracellular ROS generation in isolated human peripheral blood neutrophils were detected using DCFH-DA via flow cytometry. $n = 5$. Effects of pre-treatment with 15 mM N-acetyl cysteine (NAC) on the increased CitH3 protein expression (**b**) and release of dsDNA in human neutrophils (**c**) induced by a higher $[Cl^-]_i$. **d** Effects of pre-treatment with 1 μM GSK650394 on the increased intracellular ROS generation induced by a higher $[Cl^-]_i$. $n = 5$ per group. *ns*, $P > 0.05$; *$P < 0.05$; **$P < 0.01$; ****$P < 0.0001$.

We found that the $[Cl^-]_i$ in peripheral circulating neutrophils of both STE-ACS patients (73.6 ± 0.9 mM) and SA patients (68.5 ± 0.4 mM) was significantly increased compared to that of subjects with NCA (62.6 ± 1.1 mM) (Fig. 7a), while neutrophils in STE-ACS patients displayed the highest $[Cl^-]_i$. Correspondingly, CFTR protein expression in neutrophils of STE-ACS and SA patients was significantly lower than that of subjects with NCA, while neutrophils of STE-ACS patients displayed the lowest CFTR protein level (Fig. 7b). Plasma levels of dsDNA, MPO, and NE and neutrophil CitH3 protein expression were significantly increased in peripheral blood samples obtained from patients with STE-ACS and SA compared to those obtained from subjects with NCA. However, there were no significant differences in the levels of these four NET markers between the STE-ACS and SA groups (Fig. 7c–e). In line with increased NET levels observed in the peripheral blood of STE-ACS patients, we confirmed that proinflammatory activity within the vasculature was significantly enhanced among STE-ACS patients (Supplementary Fig. S3a–d). Peripheral circulating neutrophils obtained from STE-ACS patients expressed higher *TNF-α* and *IL-1β* levels than those from subjects with NCA, but there was no significant change in *IL-6* level (Supplementary Fig. S3a). STE-ACS patients have higher plasma levels of hs-CRP, IL-1β, and oxLDL than subjects with NCA (Supplementary Fig. S3b). TNF-α and phosphorylated NF-κB protein expressions in neutrophils of STE-ACS patients were significantly increased compared with those in neutrophils of subjects with NCA (Supplementary Fig. S3c, d). Moreover, phosphorylated SGK1 protein expression in peripheral circulating neutrophils of STE-ACS patients was significantly increased compared to that of subjects with NCA (Fig. 7f). In addition, GSK650394 administration did not affect the $[Cl^-]_i$ of freshly isolated peripheral circulating neutrophils in the NCA and STE-ACS groups (Fig. 7g), suggesting that constitutive activation of SGK1 may be a downstream signaling step of higher $[Cl^-]_i$ in neutrophils associated with STE-ACS. Moreover, $[Cl^-]_i$ elevation in neutrophils of SA or STE-ACS patients could be partially reversed by in vitro

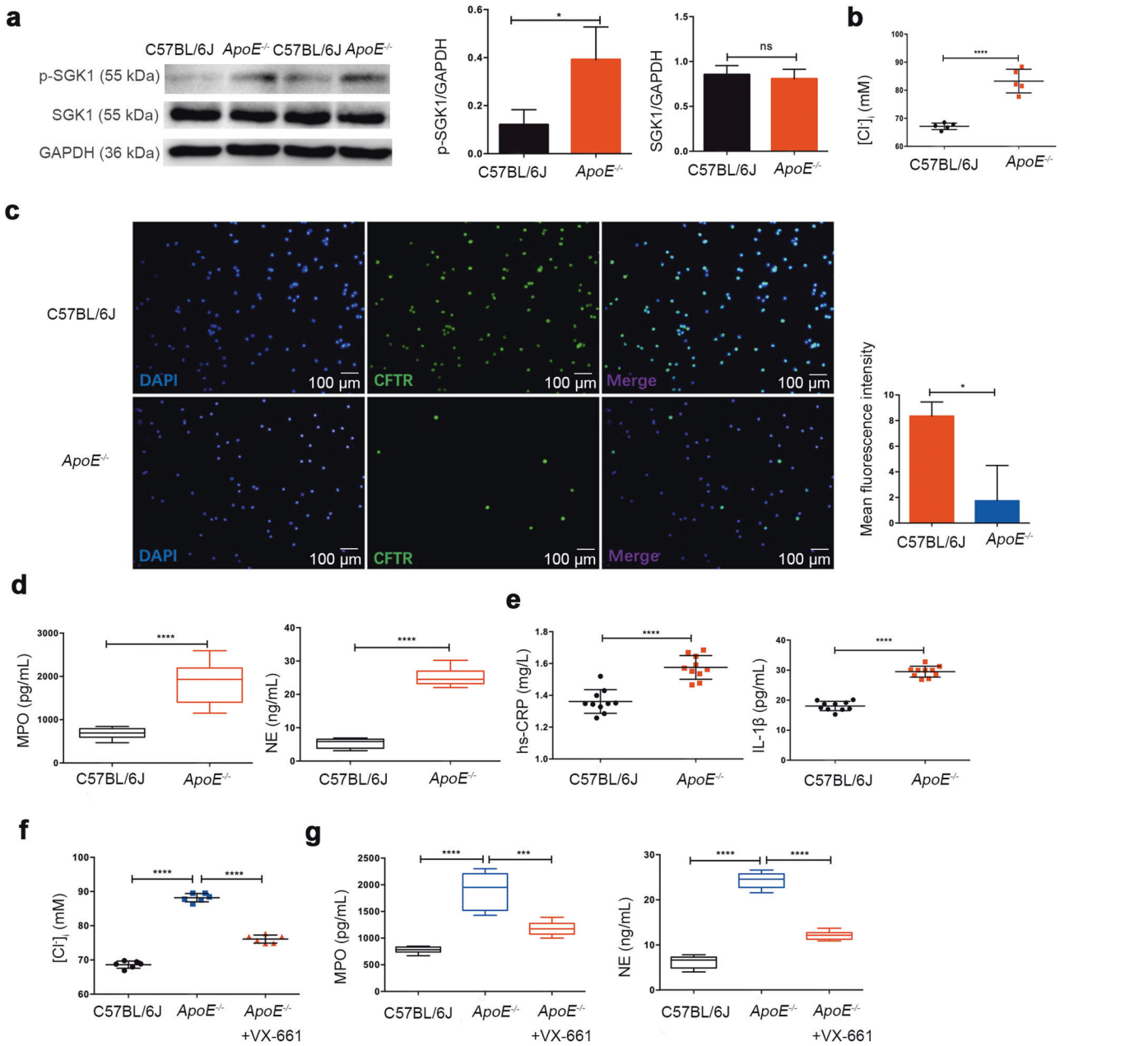

Fig. 6 Elevated neutrophil $[Cl^-]_i$, NET burden, and proinflammatory cytokine levels in the peripheral blood of atherosclerotic *ApoE*$^{-/-}$ mice on a high-fat diet. Atherosclerotic *ApoE*$^{-/-}$ mice and age-matched C57BL/6J mice were fed a high-fat diet for 16 weeks. **a** Western blotting assay of total and phosphorylated SGK1 (S422) on mouse neutrophils. **b** Measurement of $[Cl^-]_i$ with MQAE. **c** CFTR expression was analyzed via immunofluorescence staining with FITC-labeled secondary antibody (green). Scale bar = 100 μm. ELISA of plasma levels of MPO and NE (**d**) or hs-CRP and IL-1β (**e**). Effects of VX-661 (5 μM) on neutrophil $[Cl^-]_i$ (**f**) and plasma level of MPO and NE (**g**) in peripheral blood samples obtained from *ApoE*$^{-/-}$ mice. *ns*, $P > 0.05$; *$P < 0.05$; ***$P < 0.001$; ****$P < 0.0001$, $n = 5$–10 mice per group.

VX-661 treatment (Fig. 7h). VX-661 could significantly reduce NET formation (assessed via dsDNA) in peripheral blood samples obtained from patients with STE-ACS (Fig. 7i).

DISCUSSION

This is the first study to report that $[Cl^-]_i$ is increased, while CFTR protein expression is decreased, in peripheral circulating neutrophils of SA and STE-ACS patients with coincidentally enhanced NET formation, suggesting that the $[Cl^-]_i$ resulting from oxLDL stimulation or reduced CFTR function may be a novel trigger for NET formation associated with atherosclerotic cardiovascular diseases.

Recent accumulating pieces of evidence have recognized aggravated NET formation as a key driver in the pathology of ACS, where excessive NET levels contribute to the development of proinflammatory and prothrombotic milieu [4]. Therapeutic approaches that reduce NET formation, such as DNase 1 therapy and PAD4 inhibition, were found to experimentally reduce thrombosis and inflammatory responses, suggesting that NETs are important therapeutic targets for the treatment of atherosclerotic cardiovascular diseases. Although previous studies have suggested the intimate association between the Cl^- transport and neutrophil functions [30, 31], whether the alteration of $[Cl^-]_i$ occurs in neutrophils in the pathogenesis of atherosclerotic cardiovascular diseases has not been fully understood. In this

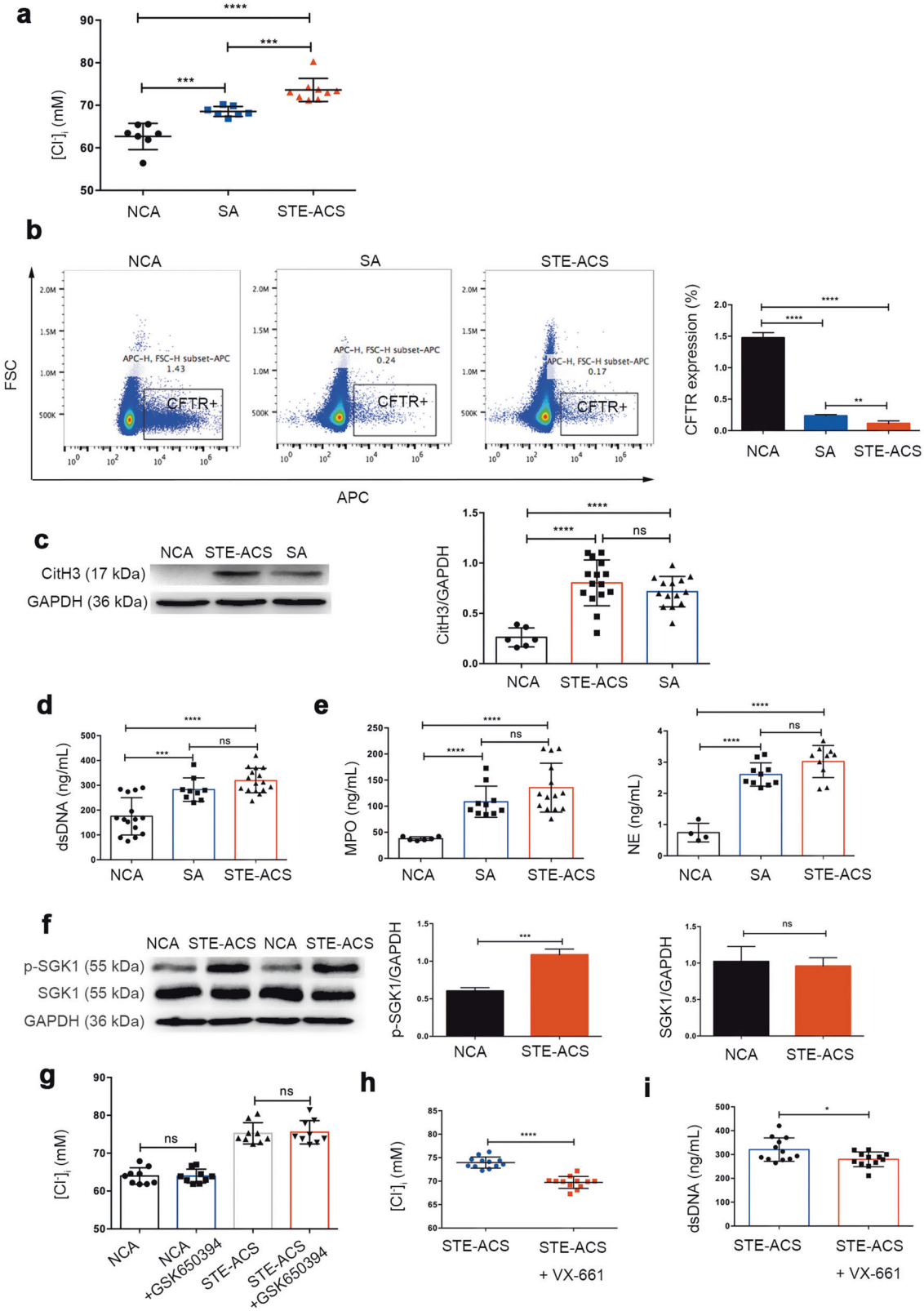

Fig. 7 Elevated NET burden in peripheral blood of SA and STE-ACS patients with alterations of neutrophil CFTR, $[Cl^-]_i$, and SGK1 activity. Peripheral blood neutrophils were collected from subjects with NCA and SA and STE-ACS patients. **a** Measurement of $[Cl^-]_i$ with MQAE (NCA, $n = 7$; SA, $n = 7$; STE-ACS, $n = 9$). **b** Flow cytometric analysis of CFTR protein expression. $n = 5$ per group. **c** Western blotting of CitH3 protein expression (NCA, $n = 6$; SA, $n = 14$; STE-ACS, $n = 15$). **d** Fluorescence probe analysis of plasma dsDNA level (NCA, $n = 15$; SA, $n = 9$; STE-ACS, $n = 15$). **e** ELISA of plasma levels of MPO and NE. **f** Western blotting assay of total and phosphorylated SGK1 on neutrophils in the NCA and STE-ACS groups. $n = 5$ per group. **g** Effects of GSK650394 (1 μM) on $[Cl^-]_i$ in neutrophils isolated from the NCA and STE-ACS groups. $n = 9$ per group. Effects of VX-661 (5 μM) on neutrophil $[Cl^-]_i$ (**h**) and plasma level of dsDNA (**i**) in peripheral blood samples obtained from STE-ACS patients. $n = 12$ per group. *ns*, $P > 0.05$; *$P < 0.05$; **$P < 0.01$, ***$P < 0.001$; ****$P < 0.0001$.

study, we found for the first time that peripheral circulating neutrophils from SA or STE-ACS patients have dramatically elevated $[Cl^-]_i$, accompanied by elevated plasma oxLDL level and NETs within the vasculature. We also observed that neutrophil $[Cl^-]_i$ was significantly increased when more NETs were formed upon stimulation with oxLDL, which could be aggravated by *CFTR* deficiency but abolished by the CFTR corrector VX-661. Finally, increased neutrophil $[Cl^-]_i$ directly triggered NET formation. These results suggest that elevated $[Cl^-]_i$ secondary to oxLDL stimulation and CFTR dysfunction may be a cause of inflammatory responses in non-infectious diseases such as cardiovascular diseases. Moreover, increased neutrophil $[Cl^-]_i$ or heightened $[Cl^-]_i$ by $CFTR_{inh}$-172 or *CFTR* knockout triggered NET formation through the upregulation of SGK1 and intracellular ROS production, while GSK650394 or NAC significantly decreased NET formation induced by oxLDL or higher $[Cl^-]_i$. These results suggest that elevated $[Cl^-]_i$ may serve as a novel "intracellular second messenger" linking extracellular disease-relevant stimuli to the downstream $[Cl^-]_i$-sensitive signaling pathways for NET formation. Our findings among patients with SA or STE-ACS support this postulation, although further investigations confirming the role of $[Cl^-]_i$-sensitive signaling in the atherosclerotic cardiovascular disease model are needed.

The alteration of $[Cl^-]_i$ resulting from defective CFTR Cl^- channel function has been reported to be important in the innate host defense against infection. As the first line of protection in the immune system, phagocytes require a continuous supply of Cl^- from neutrophils to generate a key antimicrobial ROS, HOCl [30, 31]. CF neutrophils thus exhibited reduced CFTR-mediated influx of Cl^- into phagosomes and led to subnormal levels of Cl^- in phagosomes, while pharmacological inhibition of CFTR in normal neutrophils yielded similar results. Another report of a study of CF neutrophils reinforces the important role of CFTR in neutrophil-mediated host defense [9]. Defective CFTR-mediated Cl^- transport resulted in elevated $[Cl^-]_i$ and thereby impaired degranulation and extracellular pseudomonal killing. CFTR potentiator (ivacaftor) treatment could intrinsically normalize $[Cl^-]_i$ and thereby improve degranulation and microbial killing. The results of the present study are in line with these reports, and we extended investigations into the role played by $[Cl^-]_i$ in regulating NET formation other than via phagocytosis. Our findings also extended the previously recognized pathological roles of the CFTR Cl^- channel that is not only associated with the *CFTR* gene mutant but also due to decreased endogenous CFTR expression. In our in vitro studies, oxLDL could decrease CFTR protein expression in healthy human neutrophils during NET formation, indicating that normal CFTR Cl^- channel could be altered not only by genetic *CFTR* defects, but also by cardiovascular risk factors.

Defective CFTR function due to *CFTR* mutation has been associated with increased NET formation in lung inflammation in a CF animal model via the suppression of neutrophil apoptosis [13]. Our results demonstrated that CFTR-dependent alteration of $[Cl^-]_i$ plays a role in NET formation at least partially through a $[Cl^-]_i$-SGK1 dependent signaling pathway. Therefore, our findings may provide a novel $[Cl^-]_i$-SGK1 dependent mechanism explaining how CFTR regulates NET formation.

Notably, oxLDL injection further augmented the increased $[Cl^-]_i$ in $Cftr^{-/-}$neutrophils (72.1 ± 0.6 vs 75.9 ± 0.4 mM) (Fig. 3d) and the production of proinflammatory cytokines and NET formation within the vasculature in $Cftr^{-/-}$ mice. These results suggested that other transmembrane Cl^- channels may play a role in NET formation. Some Cl^- channel proteins such as chloride voltage-gated channel 3 (ClC-3) and leucine-rich repeat-containing 8 VRAC subunit A (LRRC8A) are expressed in neutrophils [32–34]. For example, the ClC-3 Cl^- channel is important for oxidative burst and phagocytosis, suggesting that it might play a role in NET formation [35]. LRRC8A-dependent Cl^- channels largely account for the "swelling-activated" Cl^- currents in neutrophils [34], and we do not know yet whether it plays a role in regulating functional $[Cl^-]_i$ dynamics. Therefore, further investigation may be required to examine the influence of other Cl^- channels or Cl^- transporters on NET formation during the progression of cardiovascular diseases.

SGK1 is activated in inflammatory responses in some inflammatory or fibrotic diseases, including Crohn's disease and lung fibrosis [36]. In a variety of cell types, SGK1 is activated mainly through phosphorylation of Thr256 or Ser422. Recent evidence has shown that SGK1 is also a Cl^--sensitive kinase in the regulation of vascular smooth muscle cell apoptosis and airway epithelial inflammation [11, 12]. These studies reported that low $[Cl^-]_i$ or high $[Cl^-]_i$ activates SGK1, thus regulating downstream signaling pathways. *SGK1* deficiency and the SGK1 inhibitor, GSK650394, were shown to play an anti-inflammatory role in neutrophils by delaying apoptosis; therefore, SGK1 may be a potential target against neutrophil-mediated inflammatory responses. In the present study, we found that an $[Cl^-]_i$ of 100 mM significantly increased phosphorylated SGK1 (Ser422) but not total SGK1 protein expression during NET formation. Furthermore, the upregulation of phosphorylated SGK1 (Ser422) was found in oxLDL-treated human neutrophils, $Cftr^{-/-}$ neutrophils, and STE-ACS neutrophils. We, therefore, postulated that SGK1 activation could be triggered by increased $[Cl^-]_i$ resulting from oxLDL or defective CFTR function and plays a regulatory role during NET formation. We found that oxLDL-induced excessive NET formation or increase in ROS production induced by a higher $[Cl^-]_i$ in human neutrophils was almost abolished by pretreatment with GSK650394. However, the addition of GSK650394 did not affect the elevated $[Cl^-]_i$ in $Cftr^{-/-}$ neutrophils or increased $[Cl^-]_i$ following oxLDL treatment. Together, these findings suggested that SGK1 may be a mechanistic link between abnormally higher $[Cl^-]_i$ and excessive NET formation induced by oxLDL or loss of *CFTR*. Because the pharmacological approaches using GSK650394 may produce non-specific changes, further investigations of *SGK1* knockout mouse models will help elucidate the role played by SGK1 in neutrophil-mediated inflammatory responses in cardiovascular disease.

There is accumulating evidence that NETs are a potent proinflammatory signal in the development of atherosclerosis and ACS. Levels of markers of NET formation (e.g., dsDNA) are increased in the coronary thrombi of STE-ACS patients with coincidentally enhanced infarct size and occurrence of in-hospital major adverse cardiovascular events [3, 4]. Therefore, the coronary NET burden plays a role in predicting acute coronary events. However, our results demonstrated no significant difference between the SA and STE-ACS groups in terms of NET levels in peripheral blood samples, although neutrophils in STE-ACS tended to form more NETs than those in SA. This result may be due to the small number of STE-ACS patients enrolled or the lower inflammatory activity in peripheral blood than in coronary sinus blood. Notably, there were significant differences in neutrophil $[Cl^-]_i$ and CFTR protein expression between the two groups, suggesting that the hyper-inflammatory state in SA and STE-ACS might be associated with elevated $[Cl^-]_i$. Although not specifically addressed in the present study, *CFTR* deficiency or defective CFTR function are closely related to the development of neutrophil-mediated inflammation in infectious diseases; thus, the role of CFTR-mediated NET formation in cardiovascular disease models may provide interesting directions for future studies.

Recently, the Canakinumab Anti-inflammatory Thrombosis Outcomes Study provided compelling evidence of proinflammatory cytokines in cardiovascular diseases as potential therapeutic targets [37–40]. VX-661 (a CFTR corrector) has been demonstrated to promote processing and trafficking of the CFTR Cl^- channel to the cell membrane and thereby enhance CFTR-mediated Cl^- transport on CF and non-CF tissues [41, 42]. Our in vivo and in vitro studies found that VX-661 significantly reduced the NET

formation in peripheral blood samples obtained from oxLDL-injected mice, *ApoE*$^{-/-}$ atherosclerotic mice or patients with STE-ACS by restoring CFTR function and lowering $[Cl^-]_i$. This result may extend the pharmacological actions of CFTR correctors previously used solely in CF. Decreased endogenous CFTR protein expression in SA and STE-ACS neutrophils may provide a novel target for the development of anti-inflammatory therapies regulating abnormal $[Cl^-]_i$ and subsequent changes. However, we only measured neutrophil $[Cl^-]_i$ and CFTR in the peripheral blood of SA and STE-ACS patients in the present study. Further investigations using CFTR conditional knockout mice in combination with cardiovascular disease models would help address the role of CFTR-mediated $[Cl^-]_i$ in the pathological progression of cardiovascular diseases.

In summary, we demonstrated that oxLDL promoted NET formation secondary to increased neutrophil $[Cl^-]_i$. Increased $[Cl^-]_i$ or heightened $[Cl^-]_i$ induced by CFTR Cl^- channel inhibitor or *CFTR* knockout are hyper-responsive to NET formation through a $[Cl^-]_i$-sensitive SGK1 signaling pathway. Consistently, abnormally increased $[Cl^-]_i$ and decreased CFTR expression were observed in peripheral circulating neutrophils of SA and STE-ACS patients with coincidentally enhanced NET formation and proinflammatory milieu within the vasculature. Conversely, VX-661 confers anti-inflammatory activity and attenuates NET formation by reducing $[Cl^-]_i$. In conclusion, elevated $[Cl^-]_i$ functions as a novel trigger for NET formation in SA and STE-ACS patients, while defective CFTR may represent an appealing target for the development of future anti-inflammatory therapies in patients with atherosclerotic cardiovascular diseases.

ACKNOWLEDGEMENTS

This study was supported by the National Natural Science Foundation of China (Nos. 82073848, 81773722, 81903687, 61672547, 81773721, and 81803522); the Science and Technology Program of Guangzhou City (No. 201803010092; China); Guangdong Natural Science Foundation (No. 2020A1515010045; China); Guangdong Provincial Department of Science and Technology (No. 2017A020215104; China).

AUTHOR CONTRIBUTIONS

GLW, BZ, and HH designed the study. HH, CL, ML, and JW performed the experiments and analyzed the data. YZ, YSL, ZCL, ZHL, RH, RMW, and YYG assisted with the experiments. GLW, HH, and BZ wrote the manuscript. All authors have approved the final article.

ADDITIONAL INFORMATION

Supplementary information The online version contains supplementary material available at https://doi.org/10.1038/s41401-022-00911-9.

Competing interests: The authors declare no competing interests.

REFERENCES

1. Jorch SK, Kubes P. An emerging role for neutrophil extracellular traps in noninfectious disease. Nat Med. 2017;23:279–87.
2. Bonaventura A, Vecchie A, Abbate A, Montecucco F. Neutrophil extracellular traps and cardiovascular diseases: an update. Cells. 2020;9:23–48.
3. Mangold A, Alias S, Scherz T, Hofbauer M, Jakowitsch J, Panzenbock A, et al. Coronary neutrophil extracellular trap burden and deoxyribonuclease activity in ST-elevation acute coronary syndrome are predictors of ST-segment resolution and infarct size. Circ Res. 2015;116:1182–92.
4. Doring Y, Libby P, Soehnlein O. Neutrophil extracellular traps participate in cardiovascular diseases: recent experimental and clinical insights. Circ Res. 2020;126:1228–41.
5. Wang M, Yang H, Zheng LY, Zhang Z, Tang YB, Wang GL, et al. Downregulation of TMEM16A calcium-activated chloride channel contributes to cerebrovascular remodeling during hypertension by promoting basilar smooth muscle cell proliferation. Circulation. 2012;125:697–707.
6. Guan YY, Wang GL, Zhou JG. The ClC-3 Cl^- channel in cell volume regulation, proliferation and apoptosis in vascular smooth muscle cells. Trends Pharmacol Sci. 2006;27:290–6.
7. Testani JM, Hanberg JS, Arroyo JP, Brisco MA, Ter Maaten JM, Wilson FP, et al. Hypochloraemia is strongly and independently associated with mortality in patients with chronic heart failure. Eur J Heart Fail. 2016;18:660–8.
8. Naal T, Abuhalimeh B, Khirfan G, Dweik RA, Tang WHW, Tonelli AR. Serum chloride levels track with survival in patients with pulmonary arterial hypertension. Chest. 2018;154:541–9.
9. Pohl K, Hayes E, Keenan J, Henry M, Meleady P, Molloy K, et al. A neutrophil intrinsic impairment affecting Rab27a and degranulation in cystic fibrosis is corrected by CFTR potentiator therapy. Blood. 2014;124:999–1009.
10. Akong-Moore K, Chow OA, von Kockritz-Blickwede M, Nizet V. Influences of chloride and hypochlorite on neutrophil extracellular trap formation. PLoS One. 2012;7:e42984.
11. Chen BY, Huang CC, Lv XF, Zheng HQ, Zhang YJ, Sun L, et al. SGK1 mediates the hypotonic protective effect against H_2O_2-induced apoptosis of rat basilar artery smooth muscle cells by inhibiting the FOXO3a/Bim signaling pathway. Acta Pharmacol Sin. 2020;41:1073–84.
12. Zhang YL, Chen PX, Guan WJ, Guo HM, Qiu ZE, Xu JW, et al. Increased intracellular Cl^- concentration promotes ongoing inflammation in airway epithelium. Mucosal Immunol. 2018;11:1149–57.
13. Gray RD, Hardisty G, Regan KH, Smith M, Robb CT, Duffin R, et al. Delayed neutrophil apoptosis enhances NET formation in cystic fibrosis. Thorax. 2018;73:134–44.
14. Zhou L, Dey CR, Wert SE, DuVall MD, Frizzell RA, Whitsett JA. Correction of lethal intestinal defect in a mouse model of cystic fibrosis by human CFTR. Science. 1994;266:1705–8.
15. Melis N, Tauc M, Cougnon M, Bendahhou S, Giuliano S, Rubera I, et al. Revisiting CFTR inhibition: a comparative study of CFTRinh -172 and GlyH-101 inhibitors. Br J Pharmacol. 2014;171:3716–27.
16. Zhao LY, Li J, Yuan F, Li M, Zhang Q, Huang YY, et al. Xyloketal B attenuates atherosclerotic plaque formation and endothelial dysfunction in apolipoprotein e deficient mice. Mar Drugs. 2015;13:2306–26.
17. Huang W, Jiao J, Liu J, Huang M, Hu Y, Ran W, et al. MFG-E8 accelerates wound healing in diabetes by regulating "NLRP3 inflammasome-neutrophil extracellular traps" axis. Cell Death Discov. 2020;6:84.
18. Chen WL, Qian Y, Meng WF, Pang JY, Lin YC, Guan YY, et al. A novel marine compound xyloketal B protects against oxidized LDL-induced cell injury in vitro. Biochem Pharmacol. 2009;78:941–50.
19. Masuda S, Nakazawa D, Shida H, Miyoshi A, Kusunoki Y, Tomaru U, et al. NETosis markers: quest for specific, objective, and quantitative markers. Clin Chim Acta. 2016;459:89–93.
20. Kessenbrock K, Krumbholz M, Schonermarck U, Back W, Gross WL, Werb Z, et al. Netting neutrophils in autoimmune small-vessel vasculitis. Nat Med. 2009;15:623–5.
21. Sur Chowdhury C, Hahn S, Hasler P, Hoesli I, Lapaire O, Giaglis S. Elevated levels of total cell-free DNA in maternal serum samples arise from the generation of neutrophil extracellular traps. Fetal Diagn Ther. 2016;40:263–7.
22. Nakazawa D, Shida H, Tomaru U, Yoshida M, Nishio S, Atsumi T, et al. Enhanced formation and disordered regulation of NETs in myeloperoxidase-ANCA-associated microscopic polyangiitis. J Am Soc Nephrol. 2014;25:990–7.
23. Najmeh S, Cools-Lartigue J, Giannias B, Spicer J, Ferri LE. Simplified human neutrophil extracellular traps (NETs) isolation and handling. J Vis Exp. 2015;98:52687.
24. de Buhr N, von Kockritz-Blickwede M. Detection, visualization, and quantification of neutrophil extracellular traps (NETs) and NET markers. Methods Mol Biol. 2020;2087:425–42.
25. Masuda S, Shimizu S, Matsuo J, Nishibata Y, Kusunoki Y, Hattanda F, et al. Measurement of NET formation in vitro and in vivo by flow cytometry. Cytometry A. 2017;91:822–9.
26. Zeng JW, Zeng XL, Li FY, Ma MM, Yuan F, Liu J, et al. Cystic Fibrosis Transmembrane Conductance Regulator (CFTR) prevents apoptosis induced by hydrogen peroxide in basilar artery smooth muscle cells. Apoptosis. 2014;19:1317–29.
27. Awasthi D, Nagarkoti S, Kumar A, Dubey M, Singh AK, Pathak P, et al. Oxidized LDL induced extracellular trap formation in human neutrophils via TLR-PKC-IRAK-MAPK and NADPH-oxidase activation. Free Radic Biol Med. 2016;93:190–203.
28. Bomberger JM, Coutermarsh BA, Barnaby RL, Sato JD, Chapline MC, Stanton BA. Serum and glucocorticoid-inducible kinase1 increases plasma membrane wt-CFTR in human airway epithelial cells by inhibiting its endocytic retrieval. PLoS One. 2014;9:e89599.
29. Yamamoto K, Yamada H, Wakana N, Kikai M, Terada K, Wada N, et al. Augmented neutrophil extracellular traps formation promotes atherosclerosis development in socially defeated apoE$^{-/-}$ mice. Biochem Biophys Res Commun. 2018;500:490–6.
30. Wang G. Chloride flux in phagocytes. Immunol Rev. 2016;273:219–31.

31. Aiken ML, Painter RG, Zhou Y, Wang G. Chloride transport in functionally active phagosomes isolated from Human neutrophils. Free Radic Biol Med. 2012;53:2308–17.
32. Volk AP, Heise CK, Hougen JL, Artman CM, Volk KA, Wessels D, et al. ClC-3 and IClswell are required for normal neutrophil chemotaxis and shape change. J Biol Chem. 2008;283:34315–26.
33. Moreland JG, Davis AP, Matsuda JJ, Hook JS, Bailey G, Nauseef WM, et al. Endotoxin priming of neutrophils requires NADPH oxidase-generated oxidants and is regulated by the anion transporter ClC-3. J Biol Chem. 2007;282:33958–67.
34. Behe P, Foote JR, Levine AP, Platt CD, Chou J, Benavides F, et al. The LRRC8A mediated "swell activated" chloride conductance is dispensable for vacuolar homeostasis in neutrophils. Front Pharmacol. 2017;8:262.
35. Moreland JG, Davis AP, Bailey G, Nauseef WM, Lamb FS. Anion channels, including ClC-3, are required for normal neutrophil oxidative function, phagocytosis, and transendothelial migration. J Biol Chem. 2006;281:12277–88.
36. Artunc F, Lang F. Mineralocorticoid and SGK1-sensitive inflammation and tissue fibrosis. Nephron Physiol. 2014;128:35–9.
37. Ridker PM, Libby P, MacFadyen JG, Thuren T, Ballantyne C, Fonseca F, et al. Modulation of the interleukin-6 signalling pathway and incidence rates of atherosclerotic events and all-cause mortality: analyses from the Canakinumab Anti-Inflammatory Thrombosis Outcomes Study (CANTOS). Eur Heart J. 2018;39:3499–507.
38. Ridker PM, Everett BM, Thuren T, MacFadyen JG, Chang WH, Ballantyne C, et al. Antiinflammatory therapy with canakinumab for atherosclerotic disease. N Engl J Med. 2017;377:1119–31.
39. Crea F, Liuzzo G. Addressing acute coronary syndromes: new challenges and opportunities after the CANTOS Trial (Canakinumab Anti-inflammatory Thrombosis Outcomes Study). Circulation. 2018;137:1100–2.
40. Lorenzatti A, Servato ML. Role of anti-inflammatory interventions in coronary artery disease: understanding the canakinumab anti-inflammatory thrombosis outcomes study (CANTOS). Eur Cardiol. 2018;13:38–41.
41. Bratcher PE, Yadav S, Shaughnessy CA, Thornell IM, Zeitlin PL. Effect of apical chloride concentration on the measurement of responses to CFTR modulation in airway epithelia cultured from nasal brushings. Physiol Rep. 2020;8:e14603.
42. Cottrill KA, Giacalone VD, Margaroli C, Bridges RJ, Koval M, Tirouvanziam R, et al. Mechanistic analysis and significance of sphingomyelinase-mediated decreases in transepithelial CFTR currents in nHBEs. Physiol Rep. 2021;9:e15023.